Author/s:
Gao, C;Zhang, B;Hall, CR;Li, L;Chen, Y;Zeng, Y;Smith, TA;Wong, WWH

Title:
Triplet fusion upconversion using sterically protected 9,10-diphenylanthracene as the emitter

Date:
2020-03-21

Citation:
Gao, C., Zhang, B., Hall, C. R., Li, L., Chen, Y., Zeng, Y., Smith, T. A. & Wong, W. W. H. (2020). Triplet fusion upconversion using sterically protected 9,10-diphenylanthracene as the emitter. Physical Chemistry Chemical Physics, 22 (11), pp.6300-6307. https://doi.org/10.1039/c9cp06311k.

Triplet fusion upconversion using sterically protected 9,10-diphenylanthracene as the emitter

Received 00th January 20xx,
Accepted 00th January 20xx

DOI: 10.1039/x0xx00000x

Can Gao[a], Bolong Zhang[a], Christopher R. Hall[a], Li Li[b], Yeqin Chen[b], Yi Zeng[b], Trevor A. Smith[*a], Wallace W. H. Wong[*a]

Improving the efficiency of triplet fusion upconversion (TF-UC) in the solid-state is still challenging due to the aggregation and phase separation of chromophores. In this work, two 9,10-diphenylanthracene (DPA) derivatives based on the modification of the 9,10- phenyl rings with bulky isopropyl groups (bDPA-1 and bDPA-2) were used as emitters. By using platinum octaethylporphyrin (PtOEP) as the sensitizer, TF-UC performance was comprehensively investigated in 3 media: toluene solution, polyurethane thin film and nano/micro-crystals in polyvinyl alcohol matrix. Only a small difference in upconversion efficiency between the bulky DPAs and the DPA reference was observed in toluene solution and polyurethane thin film. However, a large improvement of TF-UC quantum yield was achieved in bDPA-2/PtOEP crystals (Φ_{UC} = (0.92 ± 0.05)%) with low excitation intensity threshold (52 mW cm^{-2}) compared to that of DPA/PtOEP crystals (Φ_{UC} = (0.09 ± 0.03)%). This difference was largely attributed to improved dispersibility of the PtOEP sensitizer in the bDPA-2 emitter crystals. The bulky DPAs also show excellent stability under UV irradiation with exposure to oxygen compared to DPA. These results provide a strategy for developing efficient solid-state TF-UC systems based on nano/micro-particles of emitter-sensitizer mixtures.

Introduction

Triplet fusion upconversion (TF-UC), also known as triplet-triplet annihilation upconversion (TTA-UC), was first reported by Parker and Hatchard in 1962.[1] It has attracted significant attention due to its advantages of working with non-coherent and low-power excitation, intense absorption of the excitation light and high upconversion quantum yield.[2, 3] In particular, efficient upconversion emission was obtained under excitation with an energy density of a few mW cm^{-2}, showing the possibility to utilize solar light as the excitation source.[4, 5] Furthermore, the excitation and emission wavelength of TF-UC can be easily tuned by selecting independent active upconversion components (the sensitizer and the emitter). Thus TF-UC has potential applications in photovoltaics, photocatalysis and bioimaging.[6-10] In the typical TF-UC scheme, the sensitizer absorbs a low energy photon leading to the formation of its singlet excited state, which is quickly converted to the triplet excited state through intersystem crossing (ISC). The triplets generated in the sensitizers can be transferred to the emitters through triplet-triplet energy transfer (TTET). TF occurs when two populated emitters collide, resulting in population of one ground- and one excited-state molecule of the emitter and the subsequent emission of a photon of higher energy than could be generated from the sensitizer alone. The TF-UC quantum yield (Φ_{UC}) is related to the statistical probability, f, of obtaining the emitter singlet state after annihilation of two triplet excited states, and the efficiencies of ISC (Φ_{ISC}), TTET (Φ_{TTET}), TF (Φ_{TF}) and fluorescence emission (Φ_{FL}) (Equation 1).

$$\Phi_{\mathrm{UC}} = \frac{1}{2} f \Phi_{\mathrm{ISC}} \Phi_{\mathrm{TTET}} \Phi_{\mathrm{TF}} \Phi_{\mathrm{FL}} \quad (1)$$

The simplest way to realize TF-UC is by dissolving the sensitizer and emitter in a suitable organic solvent, such as toluene,[11] benzene,[12] acetonitrile,[13] DMF,[14] etc. at an appropriate ratio. Highly efficient TF-UC with efficiency of up to 30% has been achieved in solution-based systems.[15] However, the use of volatile organic solvents is not practical for real-world applications. For incorporation of TF-UC with solar cell devices for solar harvesting applications, it is highly desirable to develop efficient solid-state upconverters suitable for use under low power irradiation and many efforts have been made to this end in recent years.[16-21] One of the key issues in solid-state TF-UC systems is the aggregation and phase separation of the chromophores. Recently, the Yanai and Kimizuka group reported a kinetically controlled crystal growth approach to improve the dispersibility of the sensitizer in emitter crystals.[19] A surfactant-assisted reprecipitation method was employed by injecting THF solutions of platinum octaethylporphyrin (PtOEP) and 9,10-diphenylanthracene (DPA) into an aqueous cetyltrimethylammonium bromide (CTAB) solution, resulting in a rapid nucleation and crystal growth. Increasing the concentration of PtOEP and DPA resulted in a faster crystal growth. Thus, a better sensitizer dispersibility was obtained at higher PtOEP/DPA concentration. Kamada and co-workers employed a simple approach

[a] ARC Centre of Excellence in Exciton Science, School of Chemistry, Bio21 Institute, The University of Melbourne, Melbourne, Australia. Email: trevoras@unimelb.edu.au, wwhwong@unimelb.edu.au.
[b] Key Laboratory of Photochemical Conversion and Optoelectronic Materials, Technical Institute of Physics and Chemistry, University of Chinese Academy of Sciences, Chinese Academy of Sciences, Beijing, China

Electronic Supplementary Information (ESI) available: [Supplementary Information file contains additional spectroscopic data]. See DOI: 10.1039/x0xx00000x

of drop casting the mixed solution of PtOEP/(DPA or DPA derivative) under rapid drying conditions to form the emitter (DPA or DPA derivative) matrix via rapid recrystallization before the PtOEP sensitizer aggregated.[20] Increased upconversion emission intensity was observed for alkyl-strapped DPA derivative/PtOEP compared to the DPA/PtOEP pair. This improved upconversion efficiency was attributed to better distribution of PtOEP in alkyl strapped DPA derivative crystals.

In this work, two DPA derivatives, bDPA-1 and bDPA-2, with ortho-substituted isopropyl groups on the phenyl rings were used as emitters for TF-UC with PtOEP as the sensitizer (Figure 1a). Direct comparison of TF-UC performance of the emitter/sensitizer pairs in toluene solution, polyurethane film and crystal dispersions in polyvinyl alcohol (PVA) were performed which has rarely been reported. The bulky DPAs showed competitive triplet energy transfer rates and TF-UC efficiencies both in solution and polyurethane solid-state films compared to the DPA reference. Interestingly, the rate of crystal formation for bDPA-2 was much slower than the DPA reference. This resulted in nanocrystals of bDPA-2 and PtOEP with Φ_{UC} close to 1% when incorporated in a PVA matrix and measured in air. The bulky DPA compounds also showed excellent stability under UV light irradiation in an aerated environment as a result of steric protection of the anthracene core.

Experimental

Materials

The bulky-DPAs were synthesized via Suzuki-Miyaura coupling according to the literature.[22] The sensitizer PtOEP was purchased from Sigma-Aldrich chemical company. The polyurethane precursors - polyol and diisocyanate – were purchased under the trade name Clear Flex 50®, from Smooth-on, Inc.

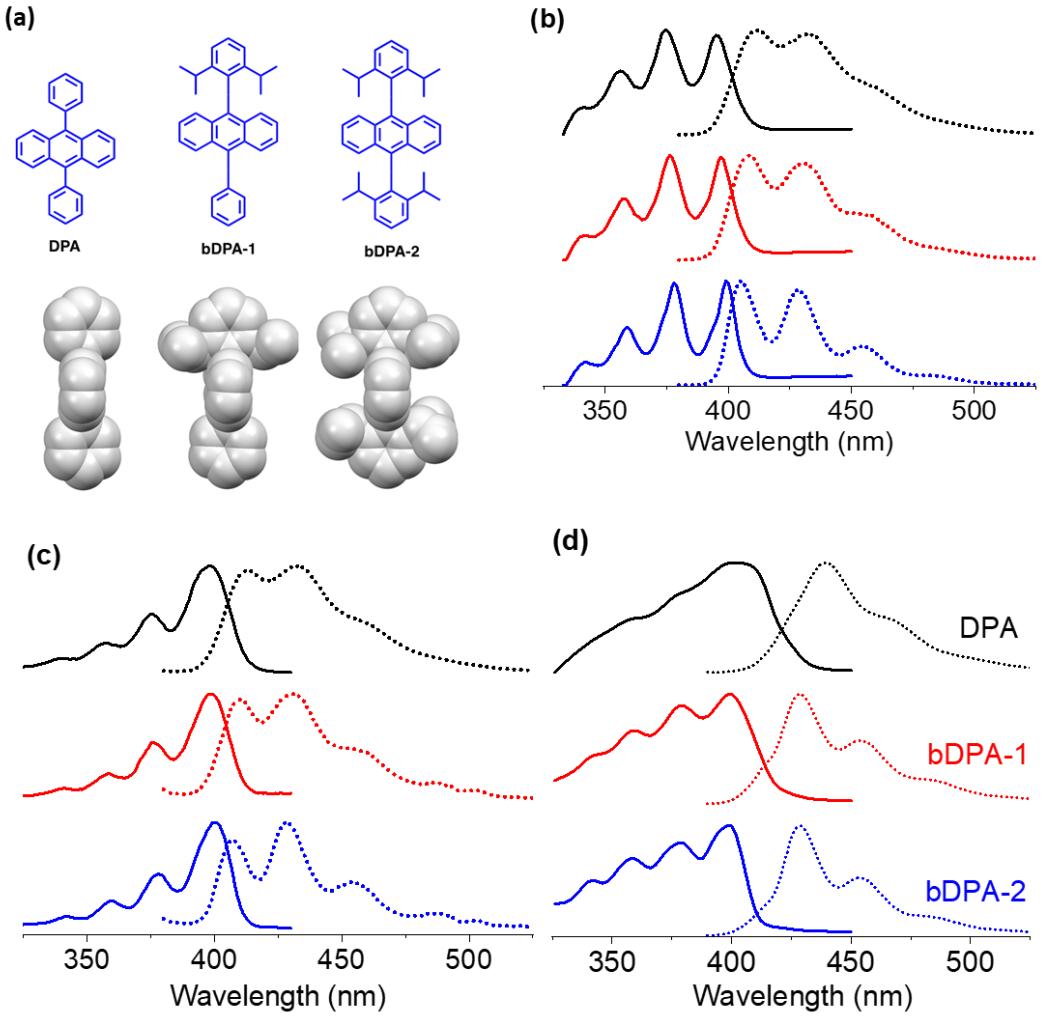

Figure 1. (a) Chemical structures and space-filling illustrations of crystal structures of DPA, bDPA-1 and bDPA-2.[22] (b) Absorption (solid traces) and photoluminescence emission (dotted traces) (λ_{ex} = 375 nm) spectra of the DPA molecules in dilute toluene solution. (c) Excitation (solid traces) (λ_{em} = 420 nm) and photoluminescence emission (dotted traces) (λ_{ex} = 375 nm) spectra of the DPA molecules in polyurethane thin films. (d) Absorption (solid traces) and photoluminescence emission (dotted traces) (λ_{ex} = 375 nm) spectra of the DPA molecules crystals

Table 1. Photophysical properties of DPA and bulky DPAs in toluene solutions.

	λ_{abs}[a] (nm)	λ_{em}[b] (nm)	ε[c] ($M^{-1}cm^{-1}$)	Φ_{FL}[d]	τ_{FL}[e] (ns)	k_{SV}[f] ($\times 10^9$ $M^{-1}s^{-1}$)	I_{th}[g] (mW cm^{-2})	Φ_{UC}[h]
DPA	373	410	4300	1.0[23]	5.5	1.2	45	5%
bDPA-1	373	410	3900	1.0	5.6	1.0	30	4.5%
bDPA-2	373	410	3500	1.0	6.2	0.6	59	4.2%

[a]Wavelength of maximum absorption. [b]Wavelength of maximum emission. [c]Molar absorption coefficient. [d]Fluorescence quantum yield. [e]Fluorescence lifetime. [f]Stern-Volmer quenching constant. [g]Excitation intensity threshold. [h]Upconversion quantum yield.

Table 2. Photophysical properties of DPA and bulky DPAs in polyurethane films.

	λ_{abs}[a] (nm)	λ_{em}[b] (nm)	τ_{FL}[c] (ns)	k_{SV}[d] ($\times 10^7$ $M^{-1}s^{-1}$)	I_{th}[e] (mW cm^{-2})	Φ_{UC}[f]
DPA	398	430	8.5	3.0	36	~1.7%
bDPA-1	399	428	8.9	2.5	36	~1.7%
bDPA-2	401	426	9.4	3.8	36	~1.7%

[a]Wavelength of maximum absorption. [b]Wavelength of maximum emission. [c]Fluorescence lifetime. [d]Stern-Volmer quenching constant. [e]Excitation intensity threshold. [f]Upconversion quantum yield.

Table 3. Photophysical properties of DPA and bulky DPAs in crystals.

	λ_{abs}[a] (nm)	λ_{em}[b] (nm)	Φ_{FL}[c] crystals	I_{th}[d] crystals	Φ_{UC}[e]
DPA	400	436	0.49	200	(0.022 ± 0.005)%
bDPA-1	400	427	0.44	110	(0.31 ± 0.02)%
bDPA-2	400	427	0.39	52	(0.92 ± 0.05)%

[a]Wavelength of maximum absorption. [b]Wavelength of maximum emission. [c]Fluorescence quantum yield. [d]Excitation intensity threshold. [e]Upconversion quantum yield.

Sample preparation

TTA-UC samples in toluene solution:

De-aerated samples in toluene were prepared using three freeze-pump-thaw cycles. The samples of DPA and the bulky DPAs for TTA upconversion measurements contained the same PtOEP (0.01 mM) and DPA (0.6 mM) concentrations. The samples containing PtOEP (0.02 mM) and DPA (0 ~ 0.08 mM) were used for a Stern-Volmer quenching measurement.

TTA-UC samples in polyurethane films:

Samples for solid-state TTA-UC measurement in polyurethane were prepared following the procedure in the literature.[24] Two different series of samples were prepared with sensitizer concentrations of 0.3 mM and 0.4 mM, and emitter concentration of 3 mM and 8 mM, respectively.

TTA-UC samples in crystals:

PtOEP (0.005 mM) and DPA/bDPAs (4 mM) in THF (4 mL) were rapidly injected into 24 mL of 10 mM sodium dodecyl sulfate (SDS) aqueous solution. After 24 hours of standing at room temperature, the precipitate was separated and purified by centrifugation at 9,000 rpm for 10 minutes and the process repeated 3 times. The precipitate was added to 200 μL 15 wt% PVA aqueous solution. The suspension was cast on a 1.25 cm × 1.25 cm × 0.1 cm glass slide and dried in a vacuum oven (60 ˚C) overnight.

Samples for stability study in PMMA films:

Samples for stability studies in PMMA were prepared by drop casting 0.1 mL of a solution of the DPA, bulky-DPAs with PMMA on top of the 1.25 cm × 1.25 cm × 0.1 cm glass slides. For each sample, three

identical samples were prepared. The samples were irradiated under a UV LED (maximum emission peak at 364 nm) with a power density of 19.8 mW cm^{-2}. The emission intensity was measured on a Varian Cary Eclipse fluorimeter every 10 minutes.

Optical measurements

Steady-state absorption and photoluminescence spectra were recorded on a Cary 50 UV-vis spectrophotometer and Varian Cary Eclipse fluorimeter, respectively. Relative Φ_{FL} values were determined by using DPA as a standard in dilute toluene solution. Fluorescence decay measurements of the emitters were performed on a time correlated single photon counting (TCSPC) setup using the frequency doubled output of a mode-locked and cavity dumped Ti:Sapphire laser (Coherent Mira 900F/APE PulseSwitch) with excitation at 405 nm. The TTA-UC quantum yields were measured under the excitation of a 532 nm CW laser in an integrating sphere (Labsphere) coupled to a Princeton Instruments Acton SP2500 spectrograph and a SPEC-10 liquid nitrogen-cooled CCD camera, and calculated according to the reported method[25]. The dispersion of crystals was dropped on a copper mesh after sonication for the transmission electron microscopy (TEM) and selected area diffraction (SAD) measurements, which were conducted on a FEI Tecnai F20 TEM instrument. Triplet decay measurements of the emitters were determined on a nanosecond flash photolysis setup by exciting at 532 nm (Ekspla NT340, operating at 10 Hz) and monitoring at 452 nm. The probe light source was MCWHLP1 Thorlabs broadband LED with DC2200 controller to generate 10ms pulses at 10 Hz, synchronized with the pump laser. The intensity of the transmitted light as a function of time was recorded on a R928 Hamamatsu PMT detector and Tektronix (TDS520) digital storage oscilloscope over 500 averages.

Results and discussion

The bulky DPAs were used for luminescent solar concentrator applications previously and showed high fluorescence quantum yield, which is ideal for TF-UC studies.[22] In addition, the influence of bulky substituents on TF-UC performance should provide more insights into the relationship between molecular structure and TF-UC process. The TF-UC performance was investigated with sensitization by PtOEP in toluene solution, polyurethane film and nano/micro-crystals in polyvinyl alcohol matrix.

TF-UC in toluene solution

The steady state absorption and photoluminescence (PL) spectra of DPA and bulky-DPAs in toluene solution are shown in Figure 1b. As the isopropyl substituents block the rotation of the phenyls, the vibronic structures in the spectra of bDPA-1 and bDPA-2 become better resolved, indicating a more rigid molecular structure.

The fluorescence quantum yield (Φ_{FL}) values of the DPA derivatives were determined in toluene solution (Table 1). With DPA as the reference (Φ_{FL} = 1.0)[23], both the bulky-DPAs show high Φ_{FL} (1.0) in toluene solution, indicating the isopropyl substituents have no influence on the Φ_{FL}. Fluorescence decay profiles of the DPAs were recorded in toluene solution (Figure S1a) and the results of the single exponential curve fit analysis are shown in Table 1. In dilute toluene solution, the fluorescence lifetimes of DPAs were around 6 ns. The small increase in lifetime from DPA to bDPA-2 can be attributed to the increased molecular rigidity reducing the non-radiative decay rate constant.

The triplet-triplet energy transfer (TTET) from the PtOEP sensitizer to DPA emitters was studied through the Stern-Volmer quenching analysis of the PtOEP phosphorescence. As shown in Figure S2b and Table 1, the Stern-Volmer quenching constants (k_{SV}) of DPA and the bulky DPAs follow the sequence of DPA (1.2×10^9 $M^{-1}s^{-1}$) > bDPA-1 (1.0×10^9 $M^{-1}s^{-1}$) > bDPA-2 (0.6×10^9 $M^{-1}s^{-1}$), which is consistent with the size of the molecules (Figure 1a). As shown in Figure 2a, the TF-UC quantum yields (Φ_{UC}) of the bulky DPAs were just over 4% with the DPA reference system at 5% (PtOEP]: 0.02 mM, [DPA]: 1 mM). The TTET and TF processes in solution are molecular diffusion-dependent, therefore, their rates are highly related to the emitter molecule size. It is clear to see from Figure 1a that the bulky DPAs are larger in size than DPA resulting in the lower Φ_{UC}. These Φ_{UC} values are different compared with some reported values for the same chromophore pair since the Φ_{UC} is dependent on the concentration as well as the ratio of the sensitizer and the emitter.[23, 26] The TF-UC excitation intensity threshold, I_{th}, is another important parameter that is used to judge the TF-UC performance.[27] As shown in Figure S2a and Table 1, all the intensity thresholds are below 60 mW cm^{-2}, which is suitable for efficient TF-UC under low excitation intensity.

TF-UC in polyurethane films

Polyurethane has been shown to be an excellent matrix for TF-UC materials due to its ability to resist oxygen penetration.[24, 28] Here we systematically study the photophysical properties and TF-UC performance of bulky DPAs in polyurethane films. One of the drawbacks of using this matrix is the propensity for aggregation of the hydrophobic dye molecules, which form micrometer sized particles that scatter the incident light[28]. To study these opaque films, we present the excitation/emission spectra instead of their absorption spectra. As shown in Figure 1c, the excitation spectra of the bDPA-1 and bDPA-2 were similar to that of DPA. As with the solution experiments, the PL spectra of bDPA-1 and bDPA-2 in polyurethane also show clear vibronic features, indicating increased molecular structure rigidity.

Fluorescence decay profiles of the DPAs in polyurethane film were recorded (Figure S1b). The decay lifetimes of the DPAs in the films were longer compared to those in solution, which can be attributed to restricted molecular motion in the solid-state reducing non-emissive decay channels. Transient absorption kinetics of the DPAs were monitored to determine the triplet lifetimes of the various emitters in polyurethane film by using PtOEP as the sensitizer (Table S1). The samples were excited at 532 nm and the triplet-triplet absorption signal was monitored at 452 nm. The transient decays are shown in Figure S9 and the lifetimes are summarized in Table S1. Both the bulky DPAs show very similar triplet lifetimes with DPA, which is appropriate for the triplet fusion upconversion process. The double-exponential nature of the triplet decay curves is attributed to aggregated (small particles) and non-aggregated forms of the

hydrophobic molecules within the hydrophilic polyurethane.[28] The molecules' motion was restricted in the polyurethane films, which resulted in the TTET and TF processes being more dependent on exciton diffusion rather than molecular diffusion. As shown in Figure S3a and Table 2, the Stern-Volmer quenching constant of bDPA-2 in the polyurethane film (3.8×10^7 $M^{-1}s^{-1}$) was slightly larger compared to that of DPA (3.0×10^7 $M^{-1}s^{-1}$) and bDPA-1 (2.5×10^7 $M^{-1}s^{-1}$), indicating less sensitizer aggregation, which resulted in more efficient TTET from PtOEP to bDPA-2. These Stern-Volmer quenching constants were two orders of magnitude smaller than the corresponding values in toluene solution, indicating reduced efficiency of the TTET process in polyurethane when molecular diffusion was severely restricted.

The excitation intensity threshold and TF-UC quantum yield of the polyurethane samples were measured with PtOEP 0.3 mM and DPA 3 mM (Figure S3a and Figure 2b). The excitation intensity thresholds of DPA and the bulky-DPAs were 36 mW cm^{-2} (Figure S3a and Table 2), lower than that in toluene solution at ~60 mW cm^{-2}. The TF-UC quantum yields were all ~1.7% (Figure 2b), indicating exciton diffusion in bulky DPAs was as efficient as that of DPA. This was not necessarily expected as the intermolecular distances and interactions can be very different for the DPA derivatives in the particulate aggregates in polyurethane. To further study the TF-UC in polyurethane films, a film with higher concentration of sensitizer (0.4 mM) and emitter (8 mM) was prepared. As shown in Figure S4a, the intensity threshold decreased to 10 mW cm^{-2} as expected. With more sensitizer in the film, more light was absorbed, thus exhibiting efficient TF-UC at lower excitation power density. The Φ_{UC} increased slightly from 1.7% (Figure 2b) to 1.9% (Figure S4b).

TF-UC in crystals

TF-UC crystals containing DPAs as the emitter and PtOEP as the sensitizer were synthesized by a surfactant-assisted dispersion method. The TEM images of TF-UC crystals are shown in Figure 3 along with the selected area diffraction (SAD) images. The DPA/PtOEP crystals (Figure 3a) were micrometer in size and non-uniform, while bDPA-1/PtOEP (Figure 3b) crystals were uniform in a

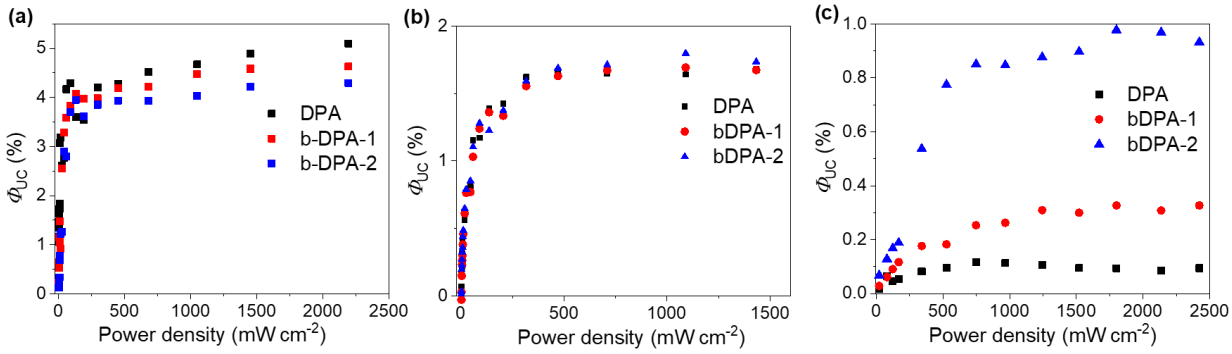

Figure 2. TF-UC quantum yield as a function of excitation power density at 532 nm (a) in toluene solution ([PtOEP]: 0.02 mM, [DPA]: 1 mM), (b) in polyurethane film. ([PtOEP]: 0.3 mM, [DPA]: 3 mM) and (c) in UC crystals in a PVA thin film.

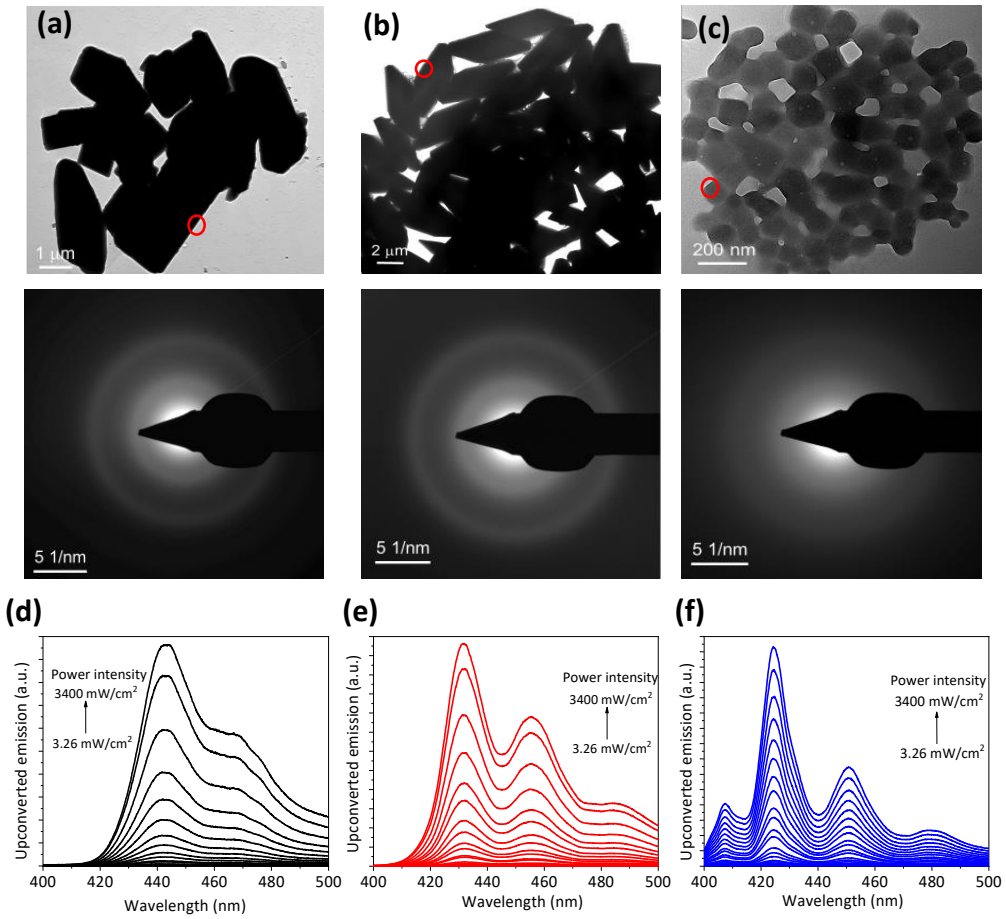

Figure 3. TEM (top) and SAD (bottom) images of TF-UC crystals (red circles represent the area for diffraction) of (a) DPA/PtOEP, (b) bDPA-1/PtOEP, (c) bDPA-2/PtOEP. Upconverted emission as a function of excitation intensity at 532 nm. (d) DPA/PtOEP, (e) bDPA-1/PtOEP, (f) bDPA-2/PtOEP.

diamond shape. The bDPA-2/PtOEP crystals were much smaller compared to DPA/PtOEP and bDPA-1/PtOEP crystals with an average size around 100 nm (Figure 3c). The SAD images of DPA/PtOEP, bDPA-1/PtOEP and bDPA-2/PtOEP reveal that these crystals were in a multicrystalline state. The crystallinity reduced from DPA/PtOEP to bDPA-2/PtOEP as indicated by reduced definition in the diffraction rings.

The absorption and PL spectra of the crystalline DPAs are shown in Figure 1d. All spectra show a small red-shift compare to in solution samples due to the molecular aggregation in the solid state. Among the emitters, DPA showed the largest red-shift, suggesting a higher degree of aggregation. To investigate the dispersed state of PtOEP molecules in emitter crystals, the Q-band absorption spectra of PtOEP were recorded (Figure S5). A dilute THF solution of PtOEP showed a Q-band absorption peak at 532 nm. The Q-band absorption of PtOEP in bDPA-1/PtOEP and DPA/PtOEP was found to be red-shifted (545 nm) compared to the THF solution of PtOEP (532 nm) due to the intermolecular interactions in the aggregates. The maximum absorption for PtOEP in bDPA-2/PtOEP was the same as in THF solution, indicating the aggregation of PtOEP was suppressed and the distribution of the sensitizer in the emitter matrix was improved. The triplet energy transfer from the sensitizer to emitter was facilitated in bDPA-2/PtOEP crystals. Consequently, efficient TF-UC with a low I_{th} value of 52 mW cm^{-2} was obtained (Figure S6 and Table 3).

The TF-UC films were prepared by blending the various DPA/PtOEP crystals with PVA and casting this mixture on a glass slide (Figure S7a). Under 532 nm CW laser excitation (Figure S7b), blue upconverted emission was observed clearly through a 500 nm short pass filter (Figure S7c). For DPA/PtOEP crystals, the maximum upconverted emission peak was at 442 nm. Blue-shifted upconverted emission was observed in bDPA-1/PtOEP and bDPA-2/PtOEP with maximum emission peaks at 430 nm and 425 nm, respectively (Figure 3d and 3e). In addition, the upconverted emission of the DPA/PtOEP and bDPAs/PtOEP crystals (Figure 3d-f) shows significant reabsorption compared to the emission spectra in dilute toluene solution (Figure 1b), while the peaks at 405 nm in the upconverted emission spectra of DPA/PtOEP and bDPAs/PtOEP crystals disappeared. This was due to their larger size as compared to the crystal size of bDPA- 2/PtOEP.

As shown in Figure 2c, the TF-UC quantum yield was (0.09 ± 0.03)% for DPA/PtOEP. This Φ_{UC} value of DPA/PtOEP was comparable to that reported in the literature of (0.022 ± 0.005)% under similar sample preparation conditions with more dilute chromophore concentration.[19] Much higher Φ_{UC} values were observed in bDPA-1/PtOEP ((0.31 ± 0.02)%) and bDPA-2/PtOEP ((0.92 ± 0.05)%), respectively. According to Equation 1, the Φ_{UC} is related to the statistical probability, *f*, of obtaining the emitter singlet state after annihilation of two triplet excited states, and the efficiencies of ISC (Φ_{ISC}), TTET (Φ_{TTET}), TF (Φ_{TF}) and fluorescence emission (Φ_{FL}). The *f* value and Φ_{ISC} can be assumed to be the same for the very similar emitter molecular structures and the identical sensitizer. With the excitation power for the maximum TF upconversion efficiency measurement being much higher than the $I_{th\ value}$ (Figure 2c and S6), the Φ_{TF} values were assumed to be the same and close to unity for the different emitter samples. From Table 3, the Φ_{FL} values in crystals decreased from DPA (0.49) to bDPA-1 (0.44) to bDPA-2 (0.39) which was opposite to the trend observed for Φ_{UC}. Therefore, the higher Φ_{UC} for the bDPA samples can be attributed to the Φ_{TTET} variation. As shown in Figure 3 and S5, the bDPA-2/PtOEP exhibited the best dispersibility of the sensitizer with the emitters. More uniform distribution of the PtOEP sensitizer in the bDPA-2 material meant more efficient TTET process affording the highest Φ_{UC} in these crystal samples. It should be noted that the benchmark Φ_{UC} values (~3%) for a DPA derivative in crystalline form was reported by Kamada et al. with the sample prepared as neat binary crystals on a quartz substrate.[20] This DPA derivative, C7-sDPA, has a similar structural design to our bDPA compounds with the anthracene chromophore protected by alkyl substituents.

The DPA/PtOEP crystals shown the highest I_{th} value (200 mW cm^{-2}) while the I_{th} value of bDPA-2/PtOEP was only (52 mW cm^{-2}) (Figure S6, Table 3). According to the above discussions, the sensitizer aggregates might be formed in DPA/PtOEP crystals, which would have a negative impact on the TTET and consequently result in a smaller Φ_{UC} value.[19] The highest dispersibility of sensitizer in bDPA-2/PtOEP (Figure S5) resulted in the lowest I_{th} value. These results demonstrated the importance of the distribution of the sensitizer in emitter crystals, which directly impacted the triplet energy transfer from sensitizer to emitter.

Stability

TF-UC is usually sensitive to molecular oxygen due to quenching of the triplet states by the triplet ground state of molecular oxygen.[29-31] Consequently, highly reactive singlet oxygen generated by this quenching process can oxidize the active chromophores in turn. For example, DPA showed degradation in the presence of singlet oxygen with the formation of endoperoxide (EP).[32, 33] To improve the photostability of DPA, Kobayashi et al. modified DPA with double alkylene straps, which protected the anthracene moiety from oxidation.[34] Usually, the TF-UC solution samples demand rigorous degassing and airtight sealing before they can be spectroscopically investigated. However, for long term real-world device application, stability against oxidation is an important consideration. Thus, stable and highly fluorescent emitter molecules are desirable for solid state TF-UC. The degradation of DPA was observed during the fluorescence emission characterization while the bulky DPA samples were observed to be more stable. Different with the photostability study of DPA derivatives in THF solution in the literature[34], in this work, the PMMA films containing DPA and the bulky DPAs were irradiated continuously under UV light for up to 40 minutes to investigate the stability of the bulky-DPAs. The variation of the integrated fluorescence emission intensity was plotted as a function of irradiation time (Figure 4). After 40 minutes irradiation, the integrated fluorescence emission intensity of DPA reduced by about 98%, becoming almost non-emissive, indicating most of the anthracene cores in DPA were oxidized. Despite the molar absorption coefficients at 364 nm for DPA, b-DPA1 and b-DPA2 being very similar (Table 1), for the bDPA-1, the integrated fluorescence emission intensity reduced approximately 70% over the same time period. Only 30% of the fluorescence emission intensity was lost for bDPA-2 in the same period, demonstrating the resistance to oxidation of this molecule compared to DPA. This significantly improved stability of bDPA-2 can be attributed to the isopropyl groups on the phenyl rings in bDPA-2 which blocked endoperoxide formation on the anthracene core. The long-term stability of emitter molecules under aerated conditions is an important factor for the application of TF-UC. Work is in progress to probe the stability of these DPA derivatives in solid state devices under TF-UC operating conditions.

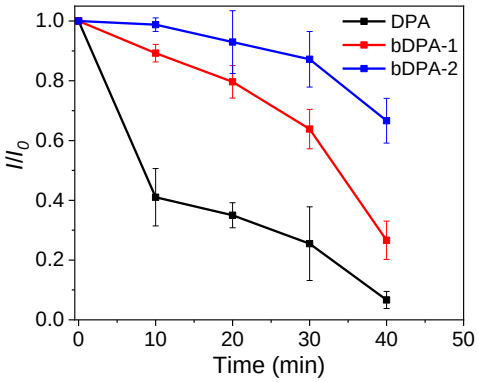

Figure 4. The variation of integrated fluorescence emission intensity of DPA and the bulky DPAs in terms of irradiation time (λ_{ex} = 364 nm, power: 19.8 mW cm^{-2}).

Conclusions

In this work, two DPA derivatives (bDPA-1 and bDPA-2) were used as emitters for TF-UC. By using PtOEP as the sensitizer, the TF-UC performance of these DPAs/PtOEP pairs was systematically studied in toluene solution, polyurethane film and crystals. Comparison across the different media revealed the TF-UC performance in polyurethane film and crystals were lower than samples in toluene solution. This can be mainly attributed to the restriction of molecular diffusion in the solid state leading to lower triplet energy transfer efficiency. The slow evaporation of the THF solvent during the formation of the polyurethane film resulted in a better mixing of the sensitizer and emitter molecules compared to crystal samples in PVA. Thus, higher Φ_{UC} was obtained in polyurethane film compared to that of the crystals. An important relationship between the molecular

structure of the DPA derivatives and their TF-UC performance was revealed. While the Φ_{UC} values for the DPA derivatives in toluene solution and polyurethane thin films were similar, bDPA-2/PtOEP crystals significantly out-performed the DPA/PtOEP reference due to better mixing of bDPA-2 and PtOEP in the sample. These results demonstrate a promising approach to improve the dispersibility of the sensitizer in emitter crystals and achieve efficient TF-UC in the solid-state. Apart from good TF-UC performance of the bulky-DPAs, they also showed improved stability under UV light irradiation, which is important for the real-world applications of TF-UC.

Conflicts of interest

There are no conflicts to declare.

Acknowledgements

This work was made possible by support from the Australian Research Council through the ARC Centre of Excellence in Exciton Science (CE170100026). WWHW and CG are further supported by Australian Renewable Energy Agency which funds the Australian Centre for Advanced Photovoltaics (ACAP). MD acknowledges International Mobility of Researchers project No. CZ.02.2.69/0.0/0.0/16_027/0008465. CG acknowledges the Albert Shimmins Fund from the University of Melbourne.

References

1. C. Parker and C. Hatchard, *J. Phys. Chem.*, 1962, **66**, 2506-2511.
2. J. Zhao, S. Ji and H. Guo, *RSC Adv.*, 2011, **1**, 937-950.
3. S. H. Lee, M. A. Ayer, R. Vadrucci, C. Weder and Y. C. Simon, *Polym. Chem.*, 2014, **5**, 6898-6904.
4. A. Monguzzi, R. Tubino and F. Meinardi, *Phys. Rev. B*, 2008, **77**, 155122.
5. J. Park, M. Xu, F. Li and H. C. Zhou, *J. Am. Chem. Soc.*, 2018, **140**, 5493-5499.
6. Y. Y. Cheng, A. Nattestad, T. F. Schulze, R. W. MacQueen, B. Fückel, K. Lips, G. G. Wallace, T. Khoury, M. J. Crossley and T. W. Schmidt, *Chem. Sci.*, 2016, **7**, 559-568.
7. J. H. Kim and J. H. Kim, *J. Am. Chem. Soc.*, 2012, **134**, 17478-17481.
8. Q. Liu, B. Yin, T. Yang, Y. Yang, Z. Shen, P. Yao and F. Li, *J. Am. Chem. Soc.*, 2013, **135**, 5029-5037.
9. Q. Liu, T. Yang, W. Feng and F. Li, *J. Am. Chem. Soc.*, 2012, **134**, 5390-5397.
10. J. Zhou, Q. Liu, W. Feng, Y. Sun and F. Li, *Chem. Rev.*, 2015, **115**, 395-465.
11. C. Gao, S. K. K. Prasad, B. Zhang, M. Dvořák, M. J. Y. Tayebjee, D. R. McCamey, T. W. Schmidt, T. A. Smith and W. W. H. Wong, *J. Phys. Chem. C*, 2019, DOI: 10.1021/acs.jpcc.9b07098.
12. T. N. Singh-Rachford, A. Haefele, R. Ziessel and F. N. Castellano, *J. Am. Chem. Soc.*, 2008, **130**, 16164-16165.
13. T. N. Singh-Rachford, R. R. Islangulov and F. N. Castellano, *J. Phys. Chem. A*, 2008, **112**, 3906-3910.
14. T. N. Singh-Rachford and F. N. Castellano, *Inorg. Chem.*, 2009, **48**, 2541-2548.
15. S. Hoseinkhani, R. Tubino, F. Meinardi and A. Monguzzi, *Phys. Chem. Chem. Phys.*, 2015, **17**, 4020-4024.
16. V. Gray, K. Moth-Poulsen, B. Albinsson and M. Abrahamsson, *Coord. Chem. Rev.*, 2018, **362**, 2560-2673.
17. N. Kimizuka, N. Yanai and M. A. Morikawa, *Langmuir*, 2016, **32**, 12304-12322.
18. B. Joarder, N. Yanai and N. Kimizuka, *J. Phys. Chem. Lett.*, 2018, **9**, 4613-4624.
19. N. Kimizuka, H. Kouno, N. Yanai and T. Ogawa, *J. Photonics Energy*, 2017, **8**, 022003.
20. K. Kamada, Y. Sakagami, T. Mizokuro, Y. Fujiwara, K. Kobayashi, K. Narushima, S. Hirata and M. Vacha, *Mater. Horiz.*, 2017, **4**, 83-87.
21. L. Li, Y. Zeng, T. Yu, J. Chen, G. Yang and Y. Li, *ChemSusChem*, 2017, **10**, 4610-4615.
22. B. Zhang, C. Gao, H. Soleimaninejad, J. M. White, T. A. Smith, D. J. Jones, K. P. Ghiggino and W. W. H. Wong, *Chem. Mater.*, 2019, **31**, 3001-3008.
23. V. Gray, D. Dzebo, A. Lundin, J. Alborzpour, M. Abrahamsson, B. Albinsson and K. Moth-Poulsen, *J. Mater. Chem. C*, 2015, **3**, 11111-11121.
24. J. Kim, F. Deng, F. N. Castellano and J. Kim, *Chem. Mater.*, 2012, **24**, 2250-2252.
25. J. C. de Mello, H. F. Wittmann and R. H. Friend, *Adv. Mater.*, 1997, **9**, 230-232.
26. A. Monguzzi, R. Tubino, S. Hoseinkhani, M. Campione and F. Meinardi, *Phys. Chem. Chem. Phys.*, 2012, **14**, 4322-4332.
27. A. Monguzzi, J. Mezyk, F. Scotognella, R. Tubino and F. Meinardi, *Phys. Rev. B*, 2008, **78**, 195112.
28. C. Gao, J. Y. Seow, B. Zhang, C. R. Hall, A. J. Tilley, J. M. White, T. A. Smith and W. W. H. Wong, *ChemPlusChem*, 2019, **84**, 746-753.
29. A. J. Svagan, D. Busko, Y. Avlasevich, G. Glasser, S. Baluschev and K. Landfester, *ACS Nano*, 2014, **8**, 8198-8207.
30. S. Wan, J. Lin, H. Su, J. Dai and W. Lu, *Chem. Commun.*, 2018, **54**, 3907-3910.
31. D. Dzebo, K. Moth-Poulsen and B. Albinsson, *Photochem. Photobiol. Sci.*, 2017, **16**, 1327-1334.
32. H. H. Wasserman, J. R. Scheffer and J. L. Cooper, *J. Am. Chem. Soc.*, 1972, **94**, 4991-4996.
33. S. H. C. Askes and B. Sylvestre, *Nat. Rev. Chem.*, 2018, **2**, 437-452.
34. Y. Fujiwara, R. Ozawa, D. Onuma, K. Suzuki, K. Yoza and K. Kobayashi, *J. Org. Chem.*, 2013, **78**, 2206-2212.